Resonance parameters of autoionizing Be $2pn\ell$ states

R. Wehlitz,[1] D. Lukić,[2] and J. B. Bluett[1,*]
[1]*Synchrotron Radiation Center, University of Wisconsin, Stoughton, Wisconsin 53589, USA*
[2]*Institute of Physics, 11001 Belgrade, Serbia and Montenegro*
(Received 4 August 2003; published 14 November 2003)

We have employed monochromatized synchrotron radiation to measure the Be^+ ion yield in the photon energy region of the Be $2pn\ell(n=3–12)$ double excitations. The energy positions of the resonances are in good agreement with a previous experiment [J. M. Esteva, G. Mehlman-Balloffet, and J. Romand, J. Quant. Spectrosc. Radiat. Transf. **12**, 1291 (1972)] and theoretical calculations. We also report the experimentally determined Fano parameters of the widths Γ and profile parameters q for the $2pns$ $(n\leqslant 8)$ resonances. The q values are about -0.54 except for $n=3$ with a clearly lower value of $-0.93(5)$.

DOI: 10.1103/PhysRevA.68.052708 PACS number(s): 32.80.Fb, 32.80.Dz

I. INTRODUCTION

While photoionization of helium has been studied thoroughly, beryllium $(1s^2 2s^2)$, the next heliumlike atom in the Periodic Table, has been investigated only marginally by comparison. Most experimental [1–3] and theoretical [4–9] papers regarding the photoionization of Be have investigated the *K*-shell region. Double excitations in the Be valence-shell region have been studied experimentally [10,11] as well as theoretically [12–19] in the past. In these experiments [10,11] vacuum sparks were used to photoexcite and -ionize Be atoms, and absorption spectra were recorded on high-sensitive film. For the calculation of the cross section in the double-excitation region different methods such as various forms of the *R*-matrix method [14,16,18], the multiconfiguration Tamm-Dancoff approximation [15], the hyperspherical method [13], a hyperspherical close-coupling calculation [19], and a multiconfiguration relativistic random-phase approximation [17] have been employed. Recently, interest has also turned to the double-photoionization process in the Be valence shell [20–22].

In general, for atomic photoexcitation resonances above the first ionization limit, autoionization becomes possible by interaction with one or more single-photoionization continua. This leads to an asymmetric resonance profile in the single-ionization cross section [23,24]. A theoretical description of this process was introduced by Fano [25] and refined later by Shore [26] and Starace [27]. There are numerous papers about double excitations in helium (see, e.g., [28,29]), which is an ideal target for studying double excitations and the subsequent autoionization. Since autoionization is a consequence of electron correlation, a measurement of the resonance profile for comparison with theory can provide important information toward our understanding of how electron correlations affect a simple system. In addition to the nonradiative decay of doubly excited states, fluorescence photons may be emitted in the decay process, and the radiative decay, in particular of long-lived states, can compete significantly with the autoionization channel [30,31].

Here we report our autoionization-profile measurements of the Be $2pns$ $(n=3–8)$ and $2pnd$ $(n=3–5)$ double excitations. Since the $1s$ electrons do not actively participate in the autoionization process, Be appears to be a system only slightly more complicated than He. However, as was found in previous investigations, it is very different from He insofar as the series of autoionizing resonances starts *immediately* above the first ionization threshold. Note that previous experiments [10,11] did not measure the photoabsorption near the threshold of the first resonance. Another difference from He is that the Be $2pns$ resonances are much broader due to a strong coupling to a rather weak continuum [12].

II. EXPERIMENT

The experiment was performed at the Synchrotron Radiation Center (SRC). Ion-yield measurements were carried out at the 4 m normal incident monochromator (NIM) beamline [32]. Photons monochromatized by a 1200 lines/mm Al-MgF_2 grating entered the experimental chamber through a glass capillary and intersected the Be vapor emerging from a resistively heated oven. The temperature of the oven was typically 1150 °C. The crucible was electrically biased to prevent thermal electrons from reaching the interaction region. The ions created were extracted by a pulsed electrical field across the interaction region, accelerated into a drift tube, and detected by a Z-stack microchannel-plate detector. By measuring the ions' flight time we obtained a time-of-flight (TOF) ion-yield spectrum. We set a time window across the Be^+ peak and, using a ratemeter, measured the count rate while scanning the photon energy. The photon flux was measured separately with an XUV100 silicon photodiode which has a known quantum efficiency. The resulting flux curve was normalized according to the electron beam current in the storage ring, which was recorded along with the Be^+ data. We also took a TOF spectrum before each photon energy scan to determine the background. The Be^+ scans were background corrected and normalized to the photon flux before further analysis. Further details of the experimental setup can be found elsewhere [33].

III. RESULTS AND DISCUSSION

Figure 1 shows our Be^+ ion-yield scan from the first ionization threshold (9.3227 eV [34]) to the first double-

*Electronic address: wehlitz@src.wisc.edu

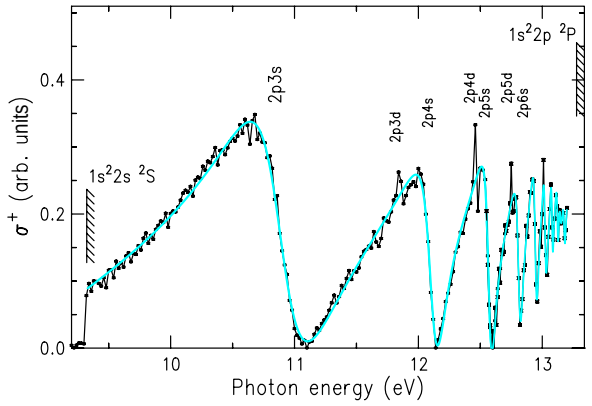

FIG. 1. Be^+ ion-yield scan across the $2pns$ and $2pnd$ resonances (circles connected by a black line) and a least-squares fit curve of Fano profiles (gray curve). Note the onset of the cross section at the first ionization threshold.

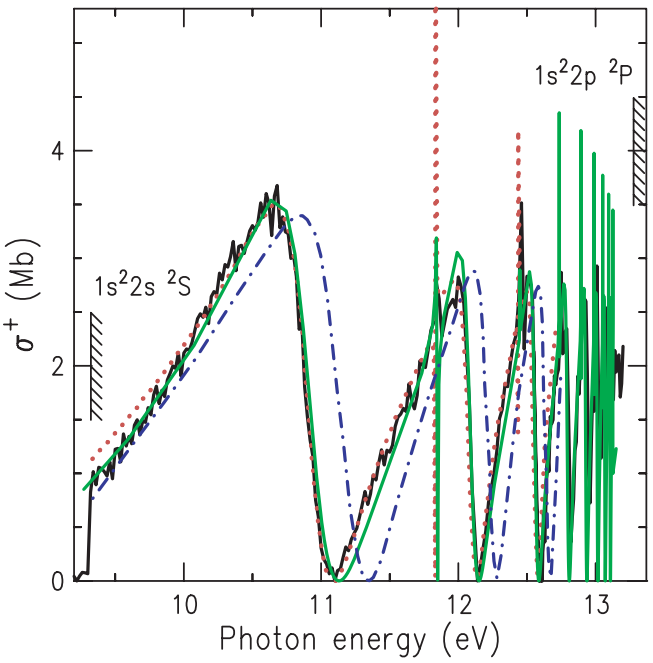

FIG. 2. Be^+ ion-yield scan across the $2pns$ and $2pnd$ resonances (solid line) together with calculated cross sections of Ref. [13] (dash-dotted line), Ref. [16] (gray solid line), and Ref. [18] (dotted line). Our experimental data were scaled to match the theoretical cross section. Note that the energy axis was slightly adjusted for the data of Greene [13] to match the energies of the $1s^22s$ and $1s^22p$ thresholds.

excitation limit Be^+ $1s^22p\ ^2P$ at 13.277 eV [35]. In the low-energy part (below 12.60 eV) of this scan the step size was 20 meV while for the higher-energy part it was 5 meV; the monochomator bandpass was 12(1) meV in both cases. The onset of the single-ionization cross section is clearly visible and appears in our scan at a photon energy of 9.32(1) eV. Note that the resonance profile of the $2p3s$ resonances starts right at the $2s^{-1}$ threshold. It is also worthwhile to mention that this measurement would not be easy to perform if we were to detect electrons instead of ions because of the resonance's close proximity to the threshold. It would require a reliable transmission function of the electron spectrometer down to 0.1 eV. Since there is only one open channel, namely, $2s \rightarrow \epsilon p$, the electron emission spectrum would be identical assuming there are no angular distribution effects except for the narrow *nd* resonances.

A comparison of our experimental data with theoretical cross sections in the $2pns$ double-excitation region (Fig. 2) shows in general a good agreement. The theoretical calculation of Greene [13] based on the hyperspherical method predicts the resonance positions at a slightly too high photon energy but reproduces the resonance shape fairly well if one scales the energy axis to match the resonance minima. The calculated cross section of Tully *et al.* [16] achieves the best match to our data, particularly below 10 eV, whereas the calculation of Kim *et al.* [18] is slightly too high near the first ionization threshold but compares favorably with our data at higher energies. Note that due to the very narrow widths of the $2pnd$ resonances the experiment does not represent them well because of a too large step size in energy.

For a quantitative analysis we have applied the Fano formula [25] with an additional slowly varying background σ_b to our data:

$$\sigma = \sigma_a \frac{(q+\epsilon)^2}{1+\epsilon^2} + \sigma_b , \tag{1}$$

where $\epsilon = 2(E-E_0)/\Gamma$. Here, q is Fano's profile parameter, which depends on the relative strength of the dipole transitions and radiationless Coulomb transitions, E is the excitation energy, E_0 is the energy position of the resonance, and Γ is the resonance width. σ_a represents the part of the continuum cross section that interacts with the discrete level. In order to fit a Fano profile to each of the $2pns$ resonances, Eq. (1) was convoluted with a Gaussian bandpass of 12 meV. Unfortunately, the $2pnd$ resonances are too narrow compared to our monochromator bandpass and energy step size to perform a fit to these resonances. Therefore, the data points that were visibly affected by the $2pnd$ resonances were removed for the fit procedure, and any interference effect of the $2pnd$ resonances on the $2pns$ resonances was assumed to be negligible.

The results of this fit procedure are summarized in Table I together with results from previous investigations. We have used our resonance positions $E_{res}(n)$ to derive the energy E_∞ of the $2pn\ell$ series limit by applying the Rydberg formula

$$E_{res}(n) = E_\infty - \mathcal{R}/(n-\delta)^2 . \tag{2}$$

Here, $\mathcal{R}$ is the Rydberg constant (13.606 eV), n is the principal quantum number, and δ is the quantum defect. Because we do not have an energy calibration more accurate than 10 meV from the onset of the single-ionization threshold (see above), we shifted all our resonance positions so that E_∞ agrees with the value 13.277 eV given by Moore [35]. We determine the quantum defect δ as 0.61(1) which is in fair agreement with the quantum defect of about 0.585, slightly varying with n, reported in Ref. [18]. Mehlman-Balloffet and Esteva [10] report a quantum defect, based on the energy

TABLE I. Our fit results for the energy position E_0, width Γ, and profile parameter q of the Be $2pns$ resonances compared to previously published values. Our resonance energies were shifted so that the $2pns$ series limit is at 13.277 eV [35].

	Energy E_0 (eV)						Width Γ (meV)				q			
n	Expt. This work	Expt. [10]	Expt. [11]	Theor. [16] [a]	Theor. [17]	Theor. [18]	Expt. This work	Theor. [18] [b]	Theor. [16]	Theor. [13]	Expt. This work	Theor. [18]	Theor. [16]	Theor. [13]
3	10.889(1)	10.7068	10.933	10.915	10.63	10.9103	531.(10)	473	606	530	−0.93(10)	−0.83	−0.91	−0.71
4	12.112(1)	11.9678	12.096	12.102	12.09	12.0918	174.(10)	162	180	168	−0.52(10)	−0.49	−0.64	−0.48
5	12.571(1)	12.5339	12.572	12.571	12.64	12.5579	77.(10)	73	78	76	−0.54(10)	−0.44	−0.48	−0.38
6	12.812(1)	12.7820	12.811	12.800	12.91	12.7911	47.(3)		42		−0.48(15)		−0.45	
7	12.944(1)	12.9219	12.945	12.932	13.06	12.9239	29.(3)		22		−0.62(15)		−0.40	
8	13.022(1)	13.0100	13.029		13.15	13.0070	16.(3)				−0.80(20)			
9	13.078(1)		13.083		13.21	13.0623	3.(5)							
10	13.123(1)		13.121		13.25	13.1009								
11	13.143(1)		13.152			13.1289								
12	13.178(1)		13.170			13.1498								

[a]This energy position was determined by a fit to the theoretical cross section data.
[b]This width is not the one reported in Ref. [18] but was determined by a fit to their data.

positions of the intensity maxima, of ca. 0.8. Note that the quantum defect changes slightly with n because it depends on the overlap of the electron's orbital with the nucleus due to the non-Coulombic potential inside the nucleus. Therefore, it is also not surprising that δ is larger in the case of Be compared to the analogous resonances in He.

As mentioned above, the $2pnd$ resonances are too narrow ($\leqslant 1$ meV [18]) to apply Eq. (1) to our data, and we determined the energy positions from the resonance maxima which are listed in Table II. We applied Eq. (2) to these energies and obtained a quantum defect for the $2pnd$ series of $\delta = -0.060(15)$, which compares favorably with the values of ca. -0.08 [18] and ca. -0.09 [10]. The smaller δ values for the $2pnd$ series compared to the $2pns$ series are easily explained by the fact that a d orbital has a smaller overlap with the nucleus than an s orbital.

In Table I we also present the resonance widths and q parameters for the $2pns$ resonances which have not been measured previously. The theoretical widths in Table I were determined by a fit using Eq. (1). Data points that obviously belong to the $2pnd$ resonances were removed before performing the fitting procedure. The resonance widths reported by Kim *et al.* [18] are always about a factor of 2.6 larger than our widths Γ because they determined the width from the inverse of the eigenphase gradient. For a more meaningful comparison of their theoretical widths with our experimental widths, we performed a fit to their cross section data using Fano profiles. In Table I we present the widths determined by our fit instead of the widths reported in Ref. [18]. Greene [13] gives only the full width at half maximum of the $2p3s$ resonance as about 1.3 eV.

TABLE II. Our energy positions (in eV) of the Be $2pnd$ resonances compared to previously published resonance positions. Our resonance energies were shifted so that the $2pns$ series limit is at 13.277 eV [35].

n	Expt. This work	Expt. [10]	Expt. [11]	Theor. [16]	Theor. [17]	Theor. [18]
3	11.840(6)	11.8623	11.855	11.840	12.03	11.8310
4	12.460(6)	12.4658	12.503	12.448	12.61	12.4374
5	12.742(6)	12.7570	12.789	12.735	12.89	12.7272
6		12.9192	12.952	12.893	13.05	12.8863

In Fig. 3 we show the width Γ as a function of the principal quantum number n as well as $\Gamma(n^*)^3$ with $n^* = n - \delta$ ($\delta = 0.61$) the effective quantum number. This product yields a constant value within the error bars for all $n \leqslant 8$. For higher n our width is not reliable because the natural width is smaller than the monochromator resolution.

Figure 4 shows our q parameters as a function of the principal quantum number n along with the theoretical q parameters. As for the widths, the theoretical q parameters were determined by a fit using Fano's formula [Eq. (1)]. While the q parameters for $n = 4$–7 appear to be constant at around -0.54, for $n = 3$ q has a distinctly smaller value of -0.9. This markedly smaller q value might be due to the fact that the underlying nonresonant cross section is not slowly

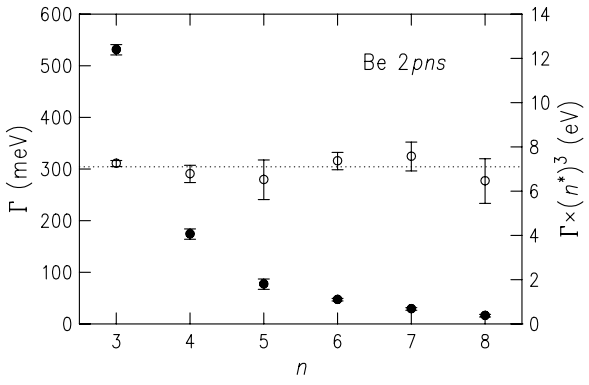

FIG. 3. Resonance widths Γ (filled circles; left-hand ordinate) of the $2pns$ resonances as a function of n. The open circles are $\Gamma \times (n^*)^3$ with $n^* = n - \delta$ the effective quantum number and δ the quantum defect (right-hand ordinate). The dotted line indicates an average value of $\Gamma \times (n^*)^3$ of 7.1 eV.

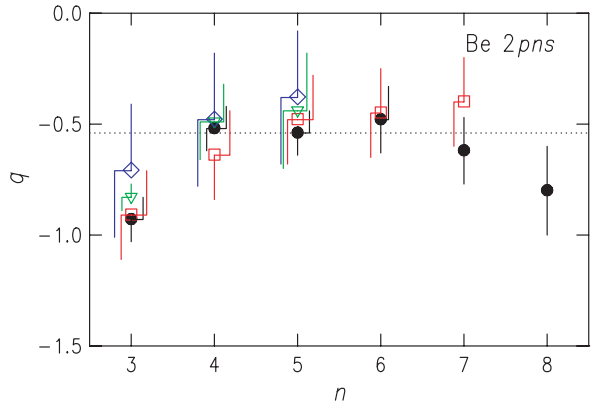

FIG. 4. Experimental (filled circles) and theoretical Fano parameters q of the $2pns$ resonances as a function of the principal quantum number n. Theoretical q values are of Ref. [16] (open squares), Ref. [13] (open diamonds), and Ref. [18] (open triangles). The dotted line represents an average q value of -0.54 for $n=4-7$.

varying—which is usually assumed—at threshold but may have a strong photon-energy dependence itself. The q parameter for $n=8$ appears to be slightly too small but may be affected by higher n resonances. The theoretical q parameters agree quite well with our experimental values; in particular the q parameters of Ref. [16] are close to our values, and confirm the distinctively smaller q value for the $2p3s$ resonance.

IV. CONCLUSION

In summary, we have measured the Be^+ photoion yield in the region of the $2pn\ell$ $(n=3-12)$ double excitations and applied the Fano formula [Eq. (1)] to the $2pns$ resonances. The energy positions of the resonances are in good agreement with a previous experiment [11] and theoretical calculations [16,18]. From the energy positions we derive a quantum defect $\delta=0.61(1)$ for the ns series and $\delta=-0.060(15)$ for the nd series. The resonance widths multiplied by $(n^*)^3$ (with n^* as the effective quantum number) remain constant and agree well with the predicted widths [13,18]. The Fano parameters q for the $2pns$ $(n\leqslant 8)$ resonances are approximately -0.54, except for the $2p3s$ resonance, which has a clearly lower q value of $-0.93(5)$. Overall, the R-matrix calculations of Tully *et al.* [16] and Kim *et al.* [18] are able to model autoionization resonances of a closed-shell atom, such as Be, very well. The hyperspherical method employed by Greene [13] also predicts the shape of the resonances fairly well, but does not calculate the right energy positions.

In future experiments, the very narrow $2pnd$ states can be investigated using a higher energy resolution to be able to compare the experimental results with theory in more detail (width and q parameter). While we do not expect any deviation from $\beta=2$ in the electron angular distribution for the $2pns$ series, the $2pnd$ series may show changes in the angular distribution, and investigations of these resonances with an electron spectrometer will give us valuable information.

ACKNOWLEDGMENTS

The authors wish to thank the SRC staff for excellent support. We also wish to thank Dr. S. B. Whitfield for critical reading of the manuscript and Dr. K. Berrington for sending us his data in numerical form. Financial support by the National Science Foundation (NSF) under Grant No. PHY-9987638 is gratefully acknowledged. One of us (D.L.) is grateful for financial support from the Ministry of Science, Technology and Development of Serbia. The SRC is operated under the NSF Grant No. DMR-0084402.

[1] M.O. Krause and C.D. Caldwell, Phys. Rev. Lett. **59**, 2736 (1987).
[2] J. Jiménez-Mier, S. Schaphorst, C.D. Caldwell, and M.O. Krause, J. Phys. B **32**, 4301 (1999).
[3] J. Jiménez-Mier, S.B. Whitfield, R. Wehlitz, and H. Díaz-Jiménez, J. Phys. B **34**, L693 (2001).
[4] H.P. Saha and C.D. Caldwell, Phys. Rev. A **40**, 7020 (1989).
[5] L. VoKy, H.E. Saraph, W. Eissner, Z.W. Liu, and H.P. Kelly, Phys. Rev. A **46**, 3945 (1992).
[6] M. Kutzner, D. Winn, and S. Mattingly, Phys. Rev. A **48**, 404 (1993).
[7] E.W.B. Dias, H.S. Chakraborty, P.C. Deshmukh, and S.T. Manson, J. Phys. B **32**, 3383 (1999).
[8] W.C. Shiu, C.-S. Hsue, and K.T. Chung, Phys. Rev. A **64**, 022714 (2001).
[9] F. Wang and B. Gou, J. Phys. B **36**, 331 (2003).
[10] G. Mehlman-Balloffet and J.M. Esteva, Astrophys. J. **157**, 945 (1969).
[11] J.M. Esteva, G. Mehlman-Balloffet, and J. Romand, J. Quant. Spectrosc. Radiat. Transf. **12**, 1291 (1972).
[12] P.L. Altick, Phys. Rev. **169**, 21 (1968).
[13] C.H. Greene, Phys. Rev. A **23**, 661 (1981).
[14] P.F. O'Mahony and C.H. Greene, Phys. Rev. A **31**, 250 (1985).
[15] V. Radojević and W.R. Johnson, Phys. Rev. A **31**, 2991 (1985).
[16] J.A. Tully, M.J. Seaton, and K.A. Berrington, J. Phys. B **23**, 3811 (1990).
[17] H.-C. Chi, K.-N. Huang, and K.T. Cheng, Phys. Rev. A **43**, 2542 (1991).
[18] D.-S. Kim, S.S. Tayal, H.-L. Zhou, and S.T. Manson, Phys. Rev. A **61**, 062701 (2000).
[19] B. Zhou and C.D. Lin, Phys. Rev. A **51**, 1286 (1995).
[20] A.S. Kheifets and I. Bray, Phys. Rev. A **65**, 012710 (2001).
[21] R. Wehlitz and S.B. Whitfield, J. Phys. B **34**, L719 (2001).
[22] J. Colgan and M.S. Pindzola, Phys. Rev. A **65**, 022709 (2002).
[23] R.P. Madden and K. Codling, Phys. Rev. Lett. **10**, 516 (1963).
[24] K. Codling, R.P. Madden, and D.L. Ederer, Phys. Rev. **155**, 26 (1967).
[25] U. Fano, Phys. Rev. **124**, 1866 (1961).
[26] B.W. Shore, Phys. Rev. **171**, 43 (1968).
[27] A.F. Starace, Phys. Rev. A **16**, 231 (1977).

[28] J.M. Rost, K. Schulz, M. Domke, and G. Kaindl, J. Phys. B **30**, 4663 (1997), and references therein.

[29] R. Püttner, B. Grémaud, D. Delande, M. Domke, M. Martins, A.S. Schlachter, and G. Kaindl, Phys. Rev. Lett. **86**, 3747 (2001).

[30] J.-E. Rubensson, C. Såthe, S. Cramm, B. Kessler, S. Stranges, R. Richter, M. Alagia, and M. Coreno, Phys. Rev. Lett. **83**, 947 (1999).

[31] K.-H. Schartner, B. Zimmermann, S. Kammer, S. Mickat, H. Schmoranzer, A. Ehresmann, H. Liebel, R. Follath, and G. Reichardt, Phys. Rev. A **64**, 040501(R) (2001), and references therein.

[32] C.H. Pruett, E.L. Brodsky, R.K. Cole, S.L. Crossley, D.B. Crossley, R.W.C. Hansen, T. Nelson, F.K. Perkins, G.C. Rogers, R.A. Rosenberg, D.J. Wallace, W.R. Winter, F.H. Middleton, A. Filipponi, and F. Zanini, Rev. Sci. Instrum. **60**, 1913 (1989).

[33] R. Wehlitz, D. Lukić, C. Koncz, and I.A. Sellin, Rev. Sci. Instrum. **73**, 1671 (2002).

[34] R. Beigang, D. Schmidt, and P.J. West, J. Phys. (Paris), Colloq. **44**, C7-229 (1983).

[35] C.E. Moore, *Atomic Energy Levels*, Natl. Bur. Stand. (U.S.) Spec. Publ. No. 467 (U.S. GPO, Washington, DC, 1949), Vol. 1.